MOBILE OPTICAL HIGH-SPEED DATA LINKS WITH SMALL TERMINALS

D. Giggenbach*
Institute of Communications and Navigation, German Aerospace Center (DLR), D-82234 Wessling

ABSTRACT

Mobile Optical Free-Space Communication (MFSO) downlinks from observation platforms in low earth orbit or in the atmosphere will allow nearly undetectable high-speed data links with small and low-power laser communication terminals. Several research institutions and companies are developing MFSO terminal technology for application in tactical and strategic communication scenarios as well as for civilian and security purposes. DLR is advancing this technology based on mature terrestrial fiber link components towards reliable and cost-effective free-space links. Successful demonstrations in the lower troposphere, the stratosphere, and from space have shown the potential of this technology. Future applications of MFSO will cover high-speed space downlinks, frequency distribution for navigation purposes, secure quantum key distribution, bidirectional links between aeronautic nodes, as well as near ground links between vehicles or ships. In this paper we will present aspects of the system design, calculate link performance limits, and show results of aeronautic and space downlink trials.

Keywords: optical free space links, laser communication terminal, atmospheric optical propagation, free-space optical high speed link, earth-observation data link, UAV data downlink, optical satellite-ground links

1. INTRODUCTION

DLR has performed different downlink trials from aeronautic and space platforms. This link technology has several advantages compared to conventional RF-links as stated in section 2. The aim is to provide a future high-speed link technology especially for missions with tight volume- and mass-constraints like UAV or micro-satellites. Results of these experiments are combined with theoretical parameter assessments in section 4 to provide link performance estimations.

All experiments have an atmospheric path section in common. The atmosphere causes distortions of the optical signal wavefront by atmospheric index-of-refraction turbulence (IRT), an effect that produces fades of the received signal. Another source for fading is miss-pointing and miss–tracking. Clouds also can cause fading or transient link blockages in satellite downlinks, which can be overcome by FEC and protocol measures. On the other side, low altitude aircraft platforms usually operate below cloud layers or do not operate at all under severe weather conditions.

*dirk.giggenbach@dlr.de; www.dlr.de

2. MOTIVATIONS AND APPLICATION SCENARIOS FOR OPTICAL DOWNLINKS

Application scenarios for optical EO-downlinks span from low-altitude UAV to satellites in LEO:

- Low-Altitude UAV or A/C (some 100m altitude) with high image resolution
- Low to medium altitude surveillance-A/C and autonomous airship (2km to 10km altitude)
- High altitude surveillance and communication platform (HAP or HALE, above 12km)
- Low-Earth-Orbit (LEO) Earth Observation (EO) Satellite (300..700km altitude)

2.1 Motivations for using optical links instead of RF or microwave downlinks

The advantages of optical links in contrast to conventional RF-links can be summarized as follows:

- High data rates (100Mbps to over 1Gbps, factor 10 to 100 compared to conventional mobile RF-links)
- Small antenna apertures / small terminal sizes (→ low weight and air-drag)
- Low transmit power, enabling low overall power consumption
- Stealth: the optical signal is nearly undetectable due to the minimized beam spread (typical few ten meters diameter at the receiver)
- Tap-proof (due to same reason of minimized signal spread)
- No regulation issues: optical links are not restricted by frequency regulation

2.2 General system setup

An optical downlink system consists of a flight terminal (FT) part and a ground station (GS) part.

The FT comprises at least: an interface to the sensor data source (which can be proprietary or a standard like Ethernet), digital data converters, the optical source with the modulated data signal, an optical amplifier, a tracking sensor, a mechanical coarse pointing assembly (CPA) to point the data beam precisely towards the GS, and diverse terminal controllers for the acquisition, tracking, and overall terminal control. Additionally, a fine pointing assembly (FPA) can be added to increase the pointing precision, and additional INS and GPS sensors can allow autonomous position and attitude determination. Typical sizes of the FT-aperture are 1cm to 10cm diameter. The signal wavelength is usually one of the classical laser wavelengths for communication purposes: 850nm, 1064nm, or 1550nm.

The GS consists of the receive telescope of typically some dm diameter, beacon sources to illuminate the FT's tracking sensor, the data receiver frontend, an optical tracking sensor, digital data converters, and a mount that allows precise pointing of the GS-telescope towards the partner.

As a major advantage of a simplex data downlink, the antenna gains can be splitted unequally between FT and GS. This means that a very small FT-aperture size – which implies a larger signal divergence as shown later - can be used when the GS compensates this with a larger aperture. With an Rx-aperture of around half a meter a very powerful system can be realized, while it still allows convenient transportation of the whole GS.

An additional RF signaling link can be used to transmit the FTs position towards the GS to allow faster initial signal acquisition. This task is not necessary with satellite downlinks as the satellite orbit is known with sufficient precision to allow initial open loop pointing of the beacons from the GS towards the satellite. Also in aeronautic scenarios, the RF signaling link is not necessary when the platform's flight path is known, e.g. when it follows pre-programmed way points.

2.3 Low altitude aeronautical downlinks

Small low-altitude platforms can be deployed very quickly on demand, e.g. as in emergency rescue situations. They can be aerodynamic (fixed- or rotary-wing) as well as aerostatic (lighter than air platforms). Their reduced field-of-regard is rather suited for observing objects or events with known location than for general wide field-of-view observation purposes. Their low to medium flight altitude on the other hand allows very high resolution images or video-surveillance with detection and tracking of individual vehicles or persons.

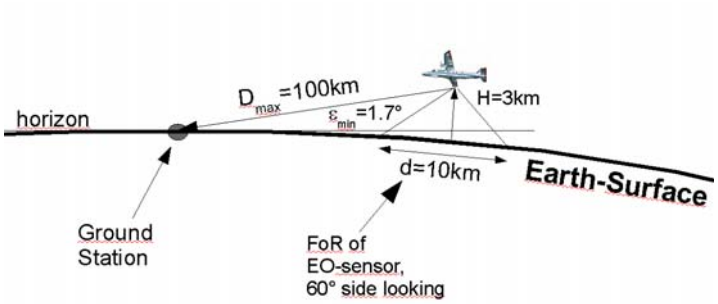

Fig. 1. Typical tropospheric optical aircraft downlink geometry [1]. Distances of more than 100km can be bridged with operating altitudes around 3km.

2.4 LEO satellite downlinks

Earth-observation satellites in polar low earth orbit (LEO) allow global observation coverage. One drawback is the limited visibility of a LEO to one ground station. This usually prevents real-time data access and requires large onboard storage of EO-data. Ground station (GS) locations near the earth's poles allow frequent contacts but operation of these GSs is aggravated. In any case, sensor operational time is mostly limited by the downlink capacity in today's systems. Therefore, higher downlink data rates directly allow increased sensor usage. With optical downlinks, the data rate can be boosted from currently 300Mbps X-Band rates to several Gbps. One solution to the visibility problem is the usage of relay satellites in GEO which see the LEO for nearly half of its orbit. But this scenario has high implementation costs and high risk of failure due to the two concatenated and long link paths. Another solution could be the use of HAPs as downlink nodes which offer greatly enhanced visibility [2]. In this paper we only deal with the more conventional and near-term scenario of direct downlinks to optical ground stations.

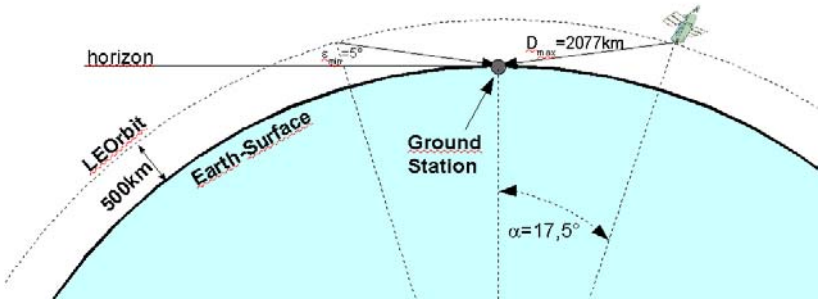

Fig. 2. Link geometry of a typical EO-Sat downlink (minimum elevation angle is 5°, ground station at sea level), the duration of one downlink is max. 9 minutes (from 5° to zenith to 5° elevation) which allows the transmission of 675GByte when using a data rate of 10Gbps [1].

For LEO space downlinks the link availability at low elevation angles is crucial for maximized system throughput, as the LEO is mostly seen near the horizon. Low elevations imply both strong signal fading and high atmospheric attenuation. Taking as an example a typical polar orbiting EO-satellite at 500km orbit altitude, the visibility analysis for one ground station in Germany shows that the satellite is seen at elevations above 30° only for 8% of its total visibility time above the horizon. For half of its visibility the satellite is seen below 8° elevation. Therefore it is of paramount importance that the optical link technology can cope with this strong-IRT channel. This applies in similar way for aeronautic downlinks which also are mostly seen at elevations below 3°.

3. CHANNEL CONSTRAINTS

The mobile atmospheric optical transmission channel poses some challenges to the data link which are not found in fixed optical fiber links. On one side there is the task of acquiring the partner terminal and keeping mutual track of its signal by precise pointing and tracking from the moving and vibrating platform. On the other the atmosphere itself causes signal attenuation by absorption and scattering and it deflects and distorts the optical beam through effects of index-of-refraction turbulence (IRT). The later is the same effect that causes the limitation in resolution of terrestrial astronomy telescopes and makes starlight twinkle at night. Only, in long horizontal free-space links, the effect is pushed to its extremes, causing fades and surges of the received intensity of more than +/-10dB.

3.1 Atmospheric attenuation in space-ground links and aeronautical downlinks

Scattering and absorption of the atmosphere's constituents cause reduction of the directed signal intensity. The different effects are Mie-scattering by droplets (haze, clouds, fog) and by dust, molecular absorption, and Rayleigh-scattering. The strength of the different effects depends on the wavelength, the altitude and the atmospheric conditions in general (volcanic activity, industrial pollution, latitude, season, subjacent terrain). Data bases deliver atmospheric attenuation coefficients and thus allow the computation of total path attenuation [3].

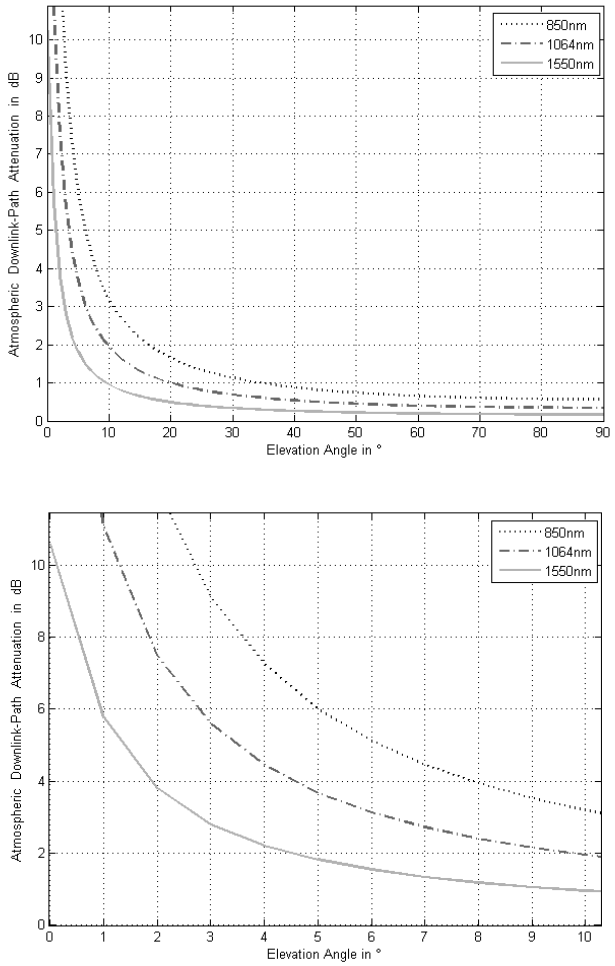

Fig. 3. Atmospheric attenuation in space downlinks for three different laser wavelengths, as a function of path elevation. Lower plot: detail below 10° elevation. The ground station is situated at 100m above sea level. Atmospheric condition is "clear sky" (no clouds, no fog) and atmospheric model is mid latitude summer with moderate volcanic activity level. Atmospheric attenuation data according to [3].

From figure 3 it becomes obvious that atmospheric attenuation is not a major issue above 20° elevation, but becomes crucial below 10°. Choosing longer signal wavelengths can save 4dB and more of attenuation at elevations below 5°, e.g. when using 1550nm instead of NIR-lasers around 850nm. This increased transmission partly compensates the lower receiver sensitivity of Indium Gallium Arsenide (InGaAs) direct detection receivers that have to be used at 1550nm, compared to silicon detectors at 850nm which are less noisy.

Other advantages when choosing 1550nm wavelength is the availability of a variety of components like laser sources, amplifiers, detectors from the terrestrial fiber communication. Also, this wavelength is approximately a factor hundred more eye-safe than 8xxnm, allowing higher radiated transmit powers.

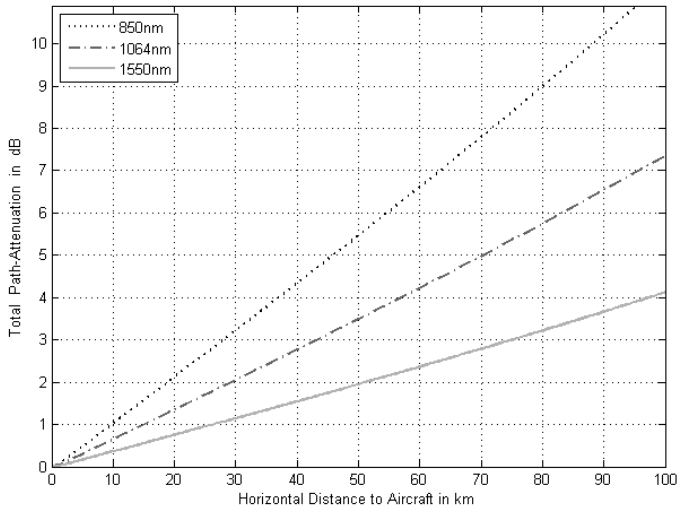

Fig. 4. Atmospheric attenuation in aeronautic downlinks as a function of horizontal distance from the aircraft to the optical ground station. The aircraft is flying at 3km altitude and the ground station is situated at 100m above sea-level, which implies a minimum elevation angle of ~2° at maximum distance. The same atmospheric conditions apply as in the figure above.

Due to the constantly low elevations seen in aeronautic downlinks, the atmospheric attenuation is in general higher than in space downlinks and taking care of the different attenuation strength is always crucial.

3.2 Link-blockage by clouds and its mitigation

The optical link can be blocked by clouds. For reliable space-downlinks, a network of optical ground stations located several hundred kilometers apart is required to enable ground station diversity in uncorrelated weather conditions. Simulations based on cloud statistics show that long-term system availabilities over 80% can be achieved with no more than four ground stations for Central Europe. For an OGS-system in less cloudy regions (e.g. in the Mediterranean) availability can easily reach above 98% [4].

3.3 Signal fading caused by atmospheric index-of-refraction turbulence (IRT), and aperture averaging

Earth's atmosphere is not a homogeneous gas volume but rather consists of cells with sizes between mm and m which have different temperature and thus different index of refraction. The variations of the index of refraction are strongest near ground and decrease with altitude. This atmospheric index-of-refraction turbulence (IRT) causes the well-known effects of intensity scintillation and wavefront distortions that have been treated thoroughly elsewhere, e.g. [5]. The high angular slew rate of the mobile link partners broadens the time-spectra of these effects [1].

As an Rx-telescope integrates the intensity over its aperture area, intensity scintillation is mitigated partially by the aperture-averaging effect of the ground station's aperture. As a precondition for an effective aperture-averaging the intensity structure sizes of the received field ρ_I must be smaller than the Rx-aperture diameter D_{Rx}. This is fulfilled in typical downlink scenarios with D_{Rx} of around half a meter and ρ_I of around 10cm. The beneficial effect of aperture averaging can only directly be exploited with modulation formats that are insensitive to wavefront distortions like e.g. Intensity-Modulation / Direct-Detection (IM/DD) or PPM, with large detector photodiodes as they are suitable for the systems described in this paper.

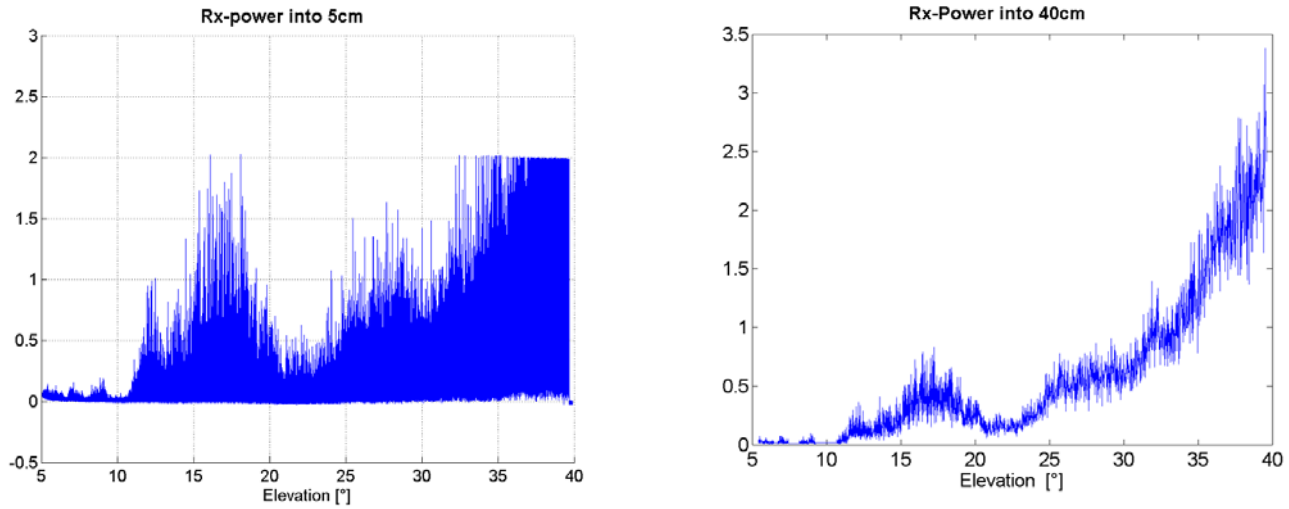

Fig. 5. Example of the aperture averaging effect during a satellite-downlink from OICETS [6]. Left: the optical power received by a small 5cm telescope which was co-aligned beside the main telescope of OGS-OP shows extreme and fast variations due to IRT; right: the power onto the 40cm telescope scintillates much less. Both graphs plotted over link path elevation, power levels in arbitrary units. Obviously the aperture-averaging of the larger telescope smoothes out strong fades and surges which can only be seen on the small aperture. The overall increase in Rx-power with elevation in both graphs is caused by the decreasing distance and atmospheric absorption, while the bump around 22° elevation was caused by a thin cloud layer. OICETS transmits a laser signal at 847nm from an orbit altitude of 610km.

4. PERFORMANCE ESTIMATION

4.1 Tracking precision and according transmitter divergence

On an aerodynamic platform, base motion disturbances caused by the engine vibrations and flight attitude instability, require high speed tracking and pointing towards the ground station. Practically, this poses a limit to the permitted transmitter divergence $\theta_{Tx\text{-}FWHM}$ which should be around four to six times the sigma of the residual pointing error, assuming gaussian distributed pointing errors (the exact value depends on how effective the FEC can recover data during moments of reduced receive power). Currently, with DLR's aeronautical terminal, pointing error values better than 300µrad are achieved by CPA-pointing only, and better values of around 100µrad are expected with the implementation of an additional FPA.

$$\theta_{Tx-FWHM} = 4 \cdot \sigma_{pointingerror} \tag{1}$$

The size of the gaussian distributed transmit field's FWHM-intensity diameter $D_{Tx\text{-}FWHM}$ (at the FT's exit aperture) defines the effective FWHM divergence angle $\theta_{Tx\text{-}FWHM}$ of the transmitter in rad according to the following formula:

$$\theta_{Tx-FWHM} = 0.44\frac{\lambda}{D_{Tx-FWHM}} \tag{2}$$

The on-axis transmitter antenna gain g_{Tx} then can be calculated in dB by

$$g_{Tx} = 20 \cdot \log\left(\frac{3.33}{\theta_{Tx-FWHM}}\right) \tag{3}$$

A certain gain of the Tx-antenna always requires a minimum Tx-aperture diameter D_{Tx}, this is an important parameter for the system design. D_{Tx} must be at least two times the $D_{Tx\text{-}FWHM}$ to allow a nearly undistorted gaussian far-field antenna pattern and it can be calculated from the two formulas above:

$$D_{Tx} \geq 2 \cdot D_{Tx-FWHM} = 0.26 \cdot \lambda \cdot 10^{g_{Tx}/20} \tag{4}$$

4.2 Free-space loss

The free-space loss (FSL) caused by the signal divergence is calculated with wavelength λ and total propagation distance L by the classical formula

$$a_{FSL} = -20 \cdot \log\left(\frac{4\pi L}{\lambda}\right) \tag{5}$$

4.3 IRT-fading loss

The classical log-normal fading model of IRT-scintillations always implies a certain fraction of signal outages. In [7] a simplified formula for calculating the IRT-losses in dB is given, which requires the received power scintillation index σ_P^2 and the fading-threshold p_{thr} as input.

$$a_{sci} \approx \left(3.3 - 5.77 \cdot \sqrt{-\ln\left(p_{thr}\right)}\right) \cdot \left(\sigma_P^{\,2}\right)^{0.4} \tag{6}$$

σ_P^2 depends on the scenario-specific intensity scintillation together with the size of the averaging effect of the Rx-aperture. Values of σ_P^2 are between 0 and 1 for low to medium turbulence and between 1 and 3 for strong turbulence cases like low elevation downlinks. σ_P^2 saturates asymptotically towards a value below 1 for very long distances. Formulas to calculate σ_P^2 can be found in [5]. The parameter p_{thr} states which time-fraction the signal may fall below the signal level required for sound data reception. Values of p_{thr} are typically chosen between 0.2 and 1E-6. This concept requires FEC specific for this fading channel to recover the data that is lost during fades, as it is described in [8]. Combined with such FEC-technique, IRT-losses can be compensated reliably.

Estimation of σ_P^2 for an aeronautic downlink can be done by using formulas 2 and 12 of [7] (which are based on theory presented in [5]) as shown in the next figure.

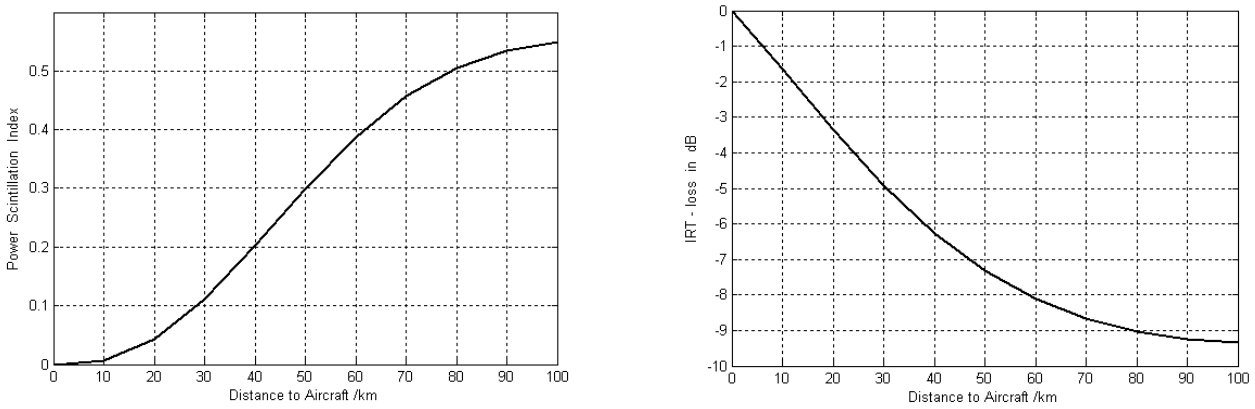

Fig. 6. Left: Power scintillation index (PSI) σ_P^2 for an aeronautical downlink to the 40cm aperture of OGS-OP, for 1550nm wavelength and with a typical turbulence strength profile. Right: According IRT-loss for p_{thr}=0.001. It can be seen that σ_P^2 and IRT-loss saturate because of scintillation saturation with long atmospheric paths.

The power scintillation index for an SGL can be calculated based on figure 12 or [6] respectively. Scaling the values measured at 847nm to another wavelength is done with the following approximation (with ε: elevation in degree, for OGS-OP with D_{Rx}=40cm):

$$\sigma_P^{\,2} \approx \frac{40}{\left(\lambda/nm\right)^{7/6}} \cdot \frac{1}{100 \cdot \varepsilon} \tag{7}$$

The formula holds only for links without saturation effect, therefore we restrict its use to elevations above 5°.

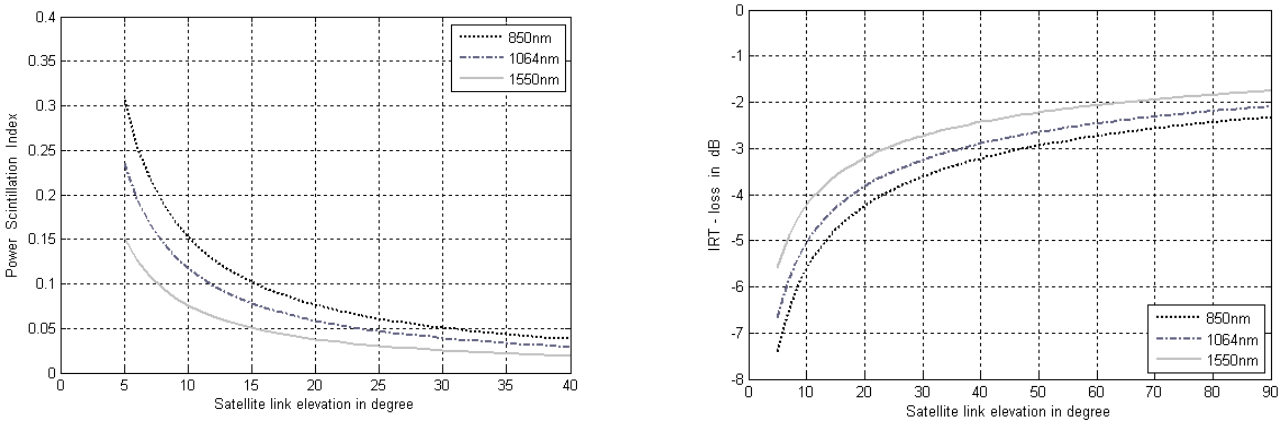

Fig. 7. Satellite downlink IRT-loss approximated from measured data for OGS-OP with its 40cm Rx-aperture (compare figure 12 and [6]). Left: power scintillation index σ_P^2 , right: IRT-loss with p_{thr}=0.001

4.4 Receive antenna gain

The aperture-area of the receiving ground telescope defines the fraction of the signal intensity which is converted into signal power in the receiver. It can be calculated in dB by the classical antenna gain formula:

$$g_{Rx} = 20 \cdot \log\left(\pi \frac{D_{Rx}}{\lambda} \right) \tag{8}$$

The above formula does not regard IRT-induced optical wavefront distortions, which can be treated as an additional IRT-fading and attenuation effect besides intensity scintillations depending on modulation formats. These field distortions will reduce the receiver sensitivity of modulation formats that require heterodyning of the received field with a local oscillator or single-mode fiber coupling. In our systems we use simple binary intensity modulation with direct detectors that act like "photon-buckets", this concept is very robust against IRT-induced wavefront distortions.

4.5 Receiver sensitivity

There exist classical limits for the sensitivity of optical data receivers, depending on the modulation format. These are given in photons per bit (Ppb) and are in average (i.e. with same numbers of zeros and ones in the binary data stream) between 36Ppb and 9Ppb for a bit error rate (BER) of 10^{-9}. Of course, these theoretical limits can not be reached in practical mobile systems, which are prone to thermal noise, background light, optical losses, sub-optimum environmental conditions, and so on. For our systems we use simple and robust Indium-Gallium-Arsenide (InGaAs) avalanche photo detectors that require an average 700Ppb for BER=10^{-7}. Although, for a precise evaluation at different data rates, bandwidth-dependent effects have to be regarded, as a simplified approximation the Ppb-number can be scaled to the transmitted data rate. For a Fast-Ethernet Link with 125Mbps channel rate this equals to 11.2nW or -49.5dBm, and for Gigabit-Ethernet with 1.25Gbps it comes to 112nW or -39,5dBm.

4.6 Link budgets

Having discussed the different link budget elements above, we evaluate the performance of the different link scenarios (wavelength is always 1550nm):

Parameter	Unit	A/C-Downlink	Sat-Downlink	Remark
Tx-power, mean	dBm	+30	+30	1W fiber amplifier
Losses Tx	dB	-2	-2	Optical and geometrical terminal losses
Tx-antenna gain	dB	+79.8	+99.8	$D_{Tx\text{-}FWHM}$ = 2mm / 20mm or $\theta_{Tx\text{-}FWHM}$ = 341µrad / 34.1µrad
Free-space loss	dB	-238	-266	100km / 2500km
Atmospheric atten.	dB	-4	-2	100km / 5° el., according to figures 3, 4
Scintillation loss	dB	-9.2	-5.5	according to (6) with p_{thr}=0.001
Miss pointing loss	dB	-3	-3	Pointing at FWHM-angle
Rx-antenna gain	dB	+118	+118	D_{Rx} = 40cm (OGS-OP)
Losses Rx	dB	-3	-3	incl. losses for tracking sensor
Background light	dB	-2	-2	Background light increases detector noise
Effective Rx-power	**dBm**	**-33.4**	**-35.7**	**mean power on APD**
Receiver sensitivity	dBm	-39.5	-39.5	1.25Gbps, 700Ppb, BER=10^{-7}
Link margin	**dB**	**+6.1**	**+3.8**	**a positive Link margin is required**

Based on the above theory, parametric system feasibility estimations can be calculated as shown in the next two figures.

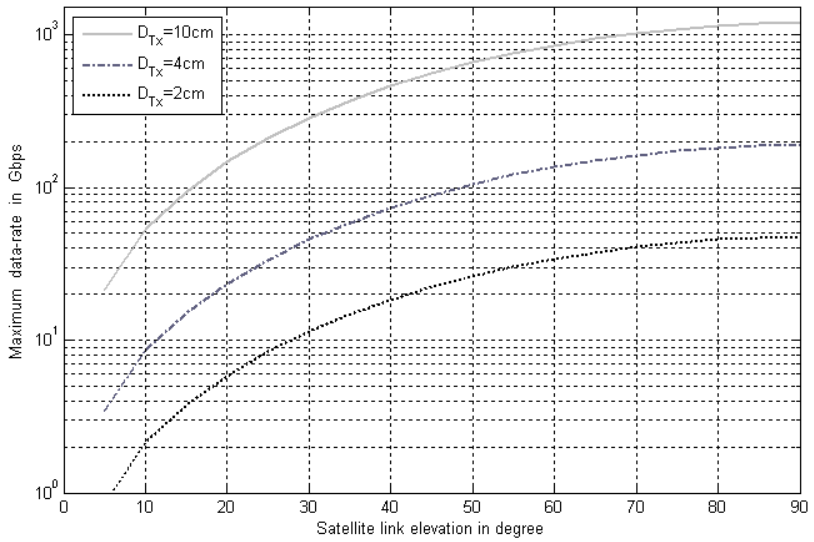

Fig. 8. LEO Satellite Downlink: maximum possible data rate over elevation, with Tx-aperture diameter D_{Tx}=2/4/10cm. Pointing error requirements according to (1), P_{Tx}=1W, wavelength=1550nm, orbit altitude=600km, no link margin.

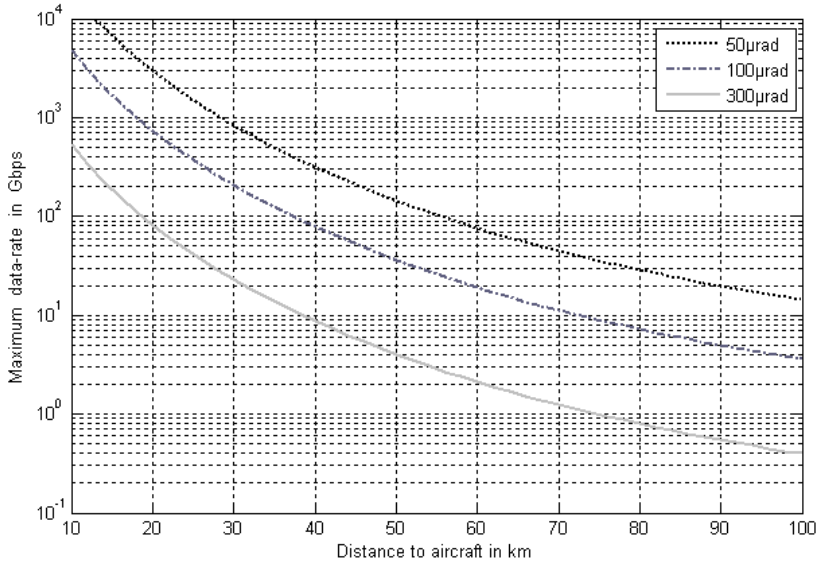

Fig. 9. A/C-Downlink: maximum possible data rate over distance, with remaining pointing error $\sigma_{pointingerror}$ = 50/100/300µrad. D_{Tx} according to (1) and (4), P_{Tx}=1W, wavelength=1550nm, A/C-altitude=3km, no link margin.

The graphs above illustrate the possible data rates based on the 700Ppb receiver sensitivity model in principle. Data-rates above approx. 10Gbps can not be realized with standard free-space direct detection systems as described before. More

sophisticated technologies like e.g. wavelength division multiplexing would be required. Obviously, due to the high link dynamic a variable data rate of the link system would be very advantageous.

4.7 FT-aperture required for tracking of the GS-beacon

Up to now it has not been considered which FT-Rx-aperture is necessary to allow reception of enough beacon power from the GS for proper tracking. Including solvable problems like scintillation compensation and background-light offset, a simple 4-quadrant tracking sensor typically requires 10pW of optical beacon power. More sophisticated and less noisy camera-like pixel arrays require even less. With GS beacon-powers of some Watts and GS pointing precision of few mrad, the received beacon-intensity at 100km at worst-case is $3\mu W/m^2$ and at an orbital distance of 2500km it becomes around $20nW/m^2$ (values calculated with 10W beacon power, 2mrad FWHM-divergence, 10dB atmospheric attenuation). Therefore, the Rx-aperture diameter at the FT needs to be at least 2mm for the aeronautic case, and 25mm for the LEO-downlink. Although this can only be a rough assessment, it clearly shows that the beacon tracking is not a driver for the aeronautic FT-aperture size, and for a satellite terminal a 1" aperture is usually acceptable.

5. VERIFICATION TRIALS

In recent years DLR has executed demonstrations of mobile optical links in several application scenarios: The stratospheric optical payload experiment (STROPEX) as part of the EU-project CAPANINA proved the feasibility of an optical high-speed (1.25Gbps) downlink from a stratospheric balloon in up to 24km altitude and 64km distance [9]. A near-ground link from a driving vehicle was tested with digital high definition video data (1.48Gbps). Here we will go into more detail of the LEO downlink trials KIODO 2006 and 2009 and the aeronautical downlink of the DLR-project ARGOS. For both experiments, DLR's Optical Ground Station Oberpfaffenhofen (OGS-OP) was used. This facility is situated on the roof-top of DLR's Institute of Communications and Navigation (see figure 10) and it consists of a 40cm Cassegrain telescope with a modular focal optical bench, different atmospheric monitoring devices, and various beacon lasers and tracking sensors [10].

Fig. 10. Optical Ground Station Oberpfaffenhofen (OGS-OP). Photograph of dome, mount, and telescope (left); The beacon lasers pointing towards JAXA's LEO satellite *OICETS* are visible on an infrared photograph due to backscatter from haze during a link experiment at night (right).

5.1 Low-altitude downlinks from aircraft: ARGOS

DLR is developing an airborne wide area observation system for monitoring of mass events, traffic, and natural disasters, called ARGOS. The observation sensors are a high resolution area sensor daylight camera and a multi-channel full polarimetric SAR system. The advantage of this system is that both, the aircraft and the receiving ground station, are quickly deployable and can supply the operational headquarter during a disaster with real-time situation awareness.

An optical IM/DD down link from one of DLR's research aircraft (a Dornier-228) with Fast-Ethernet data format and distances up to 90km was tested end of 2008 and in 2009 with pseudo-data. The FT has a 30mm aperture and transmits 125Mbps channel rate with 100mW and 1550nm wavelength [11]. By the end of 2009 live high-resolution imaging data will be transmitted to ground during a system demonstration. The project is ongoing and next development steps will be miniaturization, higher data rates (Gigabit Ethernet), and the implementation of a transportable optical ground station.

Fig. 11. Optical aircraft terminal mounted underneath DLR's Do228 (left, center of the picture); a red visualization laser of the airborne terminal pointing towards the ground station is clearly observable at approx. 10km distance (right). The co-aligned 1550nm data signal is not visible to the human eye.

5.2 Space-downlinks: KIODO 2006 / 2009

KIODO - which stands for *Kirari Optical Downlinks to Oberpfaffenhofen* – is a very successful cooperation between JAXA, NICT, and DLR, which has been ongoing since 2006. Here, IM/DD downlinks from JAXA's LEO-satellite OICETS (with second name *Kirari*) to DLR's optical ground station at Oberpfaffenhofen were performed with the aim of in-depth investigation of the optical downlink channel. Trials were executed in June 2006 and from June to September 2009. OICETS transmits pseudo-data (PRBS) at 50Mbps, directly modulated onto an 847nm laser diode with a transmit power of 100mW. A detailed presentation of KIODO-2006 can be found in [6]. One of the most important results for the performance estimation of future optical satellite-ground links is the measurement of power scintillation index σ_P^2 over elevation as shown in the next figure.

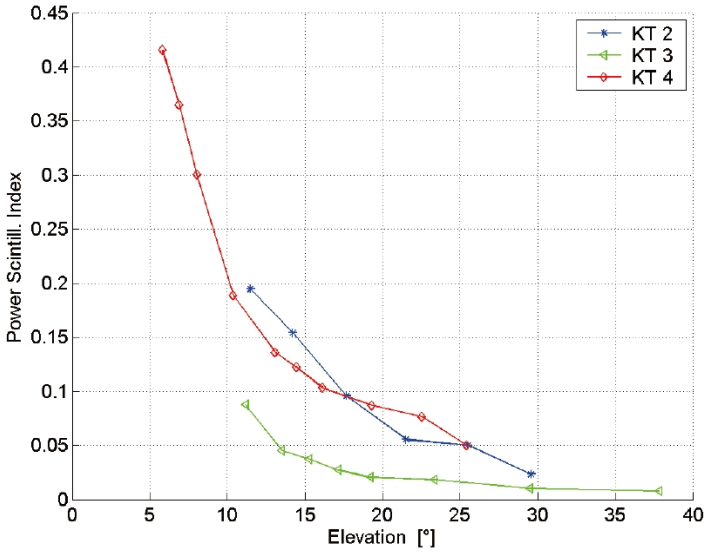

Fig. 12. Measured power scintillation index σ_P^2 of trials 2, 3, and 4 of KIODO-2006 [6]. This parameter represents the IRT-induced fading strength of the power received into the 40cm aperture of OGS-OP. The values above are for 847nm wavelength, longer wavelengths (e.g. 1550nm) will in principal show lower values of σ_P^2, compare figure 7.

6. SUMMARY AND OUTLOOK

We have shown the advantages of using mobile optical data downlinks for earth-observation applications and discussed the performance limits. Transmit terminal aperture size can be minimized to few millimetres in the aeronautical case and to few centimetres in the LEO downlink case. Data rates far above 1Gbps can be transmitted as shown by link budget estimations. Both types of downlink systems have been tested successfully in field-trials. In future developments, the data rate will be increased from Fast-Ethernet to Gigabit-Ethernet and above. Fine-pointing assemblies will in future enable more precise pointing of the FT, which again increases the overall link performance. The transmission format will be optimized to cope with the extreme fading in long horizontal link scenarios.

ACKNOWLEDGMENTS

The cooperation and kind support of Japan's JAXA and NICT in KIODO is highly appreciated. The author also wants to thank the colleagues from DLR's flight operations department at Oberpfaffenhofen for their support during ARGOS flight tests and all colleagues of DLR's Optical Communications Group who made these experiments a great success.

ABBREVIATIONS

ARGOS	Airborne wide area high altitude monitoring system
DLR	Deutsches Zentrum für Luft- und Raumfahrt (German Aerospace Center)
EO	Earth Observation
FEC	Forward Error Correction, coding technology to mitigate lost or erroneous data bits
FT	Flight Terminal
FWHM	Full-Width Half-Maximum
GS	Ground Station
HAP	High Altitude Platform
IRT	Index-of-Refraction Turbulence

JAXA	Japan Aerospace Exploration Agency
KIODO	Kirari Optical Downlink to Oberpfaffenhofen,
LEO	Low Earth Orbit
NICT	National Institute of Information and Communications Technology, Japan
OGS-OP	Optical Ground Station Oberpfaffenhofen
OICETS	Optical Inter satellite Communications Engineering and Test Satellite, by JAXA
PSI	Power Scintillation Index σ_P^2
Rx	Receive
SAR	Synthetic Aperture Radar
SGL	Satellite-Ground Link
Tx	Transmit

REFERENCES

[1] Giggenbach, D., Horwath, J., Knapek, M. "Optical Data Downlinks from Earth Observation Platforms", Proc. of SPIE 7199, 2009

[2] Giggenbach, D. Epple, B., Horwath, J., Moll, F., "Optical Satellite Downlinks to Optical Ground Stations and High-Altitude Platforms", in Advances in Mobile and Wireless Communications: Views of the 16th IST Mobile and Wireless Communication Summit, Springer, 2008

[3] Mayer, B., Shabdanov, S., Giggenbach, D., "DLR-internal electronic data base of atmospheric absorption coefficients", DLR-Oberpfaffenhofen, 2002, based on: G.P. Anderson, et al, "AFGL Atmospheric Constituent Profiles (0-120 km)", AFGL-TR-86-0110, Hanscom Air Force Base, 1986

[4] Moll, F., Knapek, M., "Wavelength Selection Criteria and Link Availability due to Cloud Coverage Statistics and Attenuation affecting Satellite, Aerial, and Downlink Scenarios", Proc. of SPIE 6709, 2007

[5] L.C. Andrews, R.L. Phillips, "Laser Beam Propagation through Random Media - Second Edition", SPIE-Press, Bellingham, 2005

[6] Jono, T., Takayama, Y., Perlot, N., et al, "Report on DLR-JAXA Joint Experiment: The Kirari Optical Downlink to Oberpfaffenhofen (KIODO)", JAXA, ISSN 1349-1121, 2007

[7] Giggenbach, D., Henniger, H., "Fading-loss assessment in atmospheric free-space optical communication links with on-off keying", Optical Engineering 47 (4), April 2008

[8] Henniger, H., Gonzalez, A., "Transmission Scheme and Error Protection for Simplex Long-Distance Atmospheric FSO Systems", Special issue of the Mediterranean Journal of Electronics and Communications on Hybrid RF and Optical Wireless Communications, 2006

[9] Horwath, J., Perlot, N., Knapek., M, Moll, F., "Experimental verification of optical backhaul links for high-altitude platform networks: Atmospheric turbulence and downlink availability", International Journal of Satellite Communications and Networking, 25 (5), 2007

[10] Knapek, M., Horwath, J., Perlot, N., Wilkerson, B., "The DLR Ground Station in the Optical Payload Experiment (STROPEX) - Results of the Atmospheric Measurement Instruments", Proc. of SPIE 6304, 2006

[11] Horwath, J., Fuchs., C., "Aircraft to Ground Unidirectional Laser-Comm. Terminal for High Resolution Sensors", Proc. of SPIE 7199, 2009